

Benchmark Experiments for Bulk and Maze Shielding Using Activation Detectors with 24-GeV/c Protons at CERN/CHARM

Noriaki Nakao, Toshiya Sanami, Tsuyoshi Kajimoto, Robert Froeschl, Davide Bozzato, Elpida Iliopoulou, Angelo Infantino, Hiroshi Yashima, Eunji Lee, Takahiro Oyama, Masayuki Hagiwara, Seiji Nagaguro, Tetsuro Matsumoto, Akihiko Masuda, Yoshitomo Uwamino, Stefan Roesler & Markus Brugger

To cite this article: Noriaki Nakao, Toshiya Sanami, Tsuyoshi Kajimoto, Robert Froeschl, Davide Bozzato, Elpida Iliopoulou, Angelo Infantino, Hiroshi Yashima, Eunji Lee, Takahiro Oyama, Masayuki Hagiwara, Seiji Nagaguro, Tetsuro Matsumoto, Akihiko Masuda, Yoshitomo Uwamino, Stefan Roesler & Markus Brugger (2024) Benchmark Experiments for Bulk and Maze Shielding Using Activation Detectors with 24-GeV/c Protons at CERN/CHARM, Nuclear Science and Engineering, 198:2, 336-347, DOI: [10.1080/00295639.2023.2196228](https://doi.org/10.1080/00295639.2023.2196228)

To link to this article: <https://doi.org/10.1080/00295639.2023.2196228>



© 2023 The Author(s). Published with license by Taylor & Francis Group, LLC.



Published online: 08 May 2023.



Submit your article to this journal [↗](#)



Article views: 1874



View related articles [↗](#)



View Crossmark data [↗](#)



Benchmark Experiments for Bulk and Maze Shielding Using Activation Detectors with 24-GeV/c Protons at CERN/CHARM

Noriaki Nakao,^{a*} Toshiya Sanami,^b Tsuyoshi Kajimoto,^c Robert Froeschl,^d Davide Bozzato,^{d,e} Elpida Iliopoulou,^{d†} Angelo Infantino,^d Hiroshi Yashima,^f Eunji Lee,^{b,g} Takahiro Oyama,^b Masayuki Hagiwara,^{b‡} Seiji Nagaguro,^b Tetsuro Matsumoto,^h Akihiko Masuda,^h Yoshitomo Uwamino,^{a§} Stefan Roesler,^d and Markus Brugger^d

^aShimizu Corporation, Institute of Technology, 3-4-7, Etchujima, Koto-ku, Tokyo 135-8530, Japan

^bHigh Energy Accelerator Research Organization (KEK), 1-1, Oho, Tsukuba, Ibaraki 305-0801, Japan

^cHiroshima University, 1-4-1, Kagamiyama, Higashi-Hiroshima, Hiroshima 739-8527, Japan

^dCERN, 1211 Geneva 23, Switzerland

^eKarlsruher Institut für Technologie (KIT), Kaiserstraße 12, 76131 Karlsruhe, Germany

^fKyoto University (KURNS), 2-1010, Asashiro-Nishi, Kumatori-cho, Sennan-gun, Osaka 590-0494, Japan

^gKyushu University, 744 Motoooka, Nishi-ku, Fukuoka 819-0395, Japan

^hNational Institute of Advanced Industrial Science and Technology (AIST), 1-1-1, Umezono, Tsukuba, Ibaraki 305-8568, Japan

Received November 28, 2022

Accepted for Publication March 23, 2023

Abstract — Measurements of high-energy neutrons through shield penetration and maze streaming were performed at the Conseil Européen pour la Recherche Nucléaire (CERN) High-energy Accelerator Mixed-Field (CHARM) facility. The protons of 24 GeV/c were injected onto a 50-cm-thick copper target and the released neutrons were transmitted through shields and a maze in the facility. The transmitted neutrons in the shield and maze were measured using activation detectors placed behind various materials and thicknesses of the shields and at several locations in the maze. From the radionuclide production rates in the activation detectors, the attenuation profiles through the shield thickness and along the maze were obtained for the reactions of $^{209}\text{Bi}(n, xn)^{210-x}\text{Bi}$ ($x = 4-9$), $^{27}\text{Al}(n, \alpha)^{24}\text{Na}$, $^{115}\text{In}(n, n')^{115m}\text{In}$, and $^{12}\text{C}(n, 2n)^{11}\text{C}$. Monte Carlo simulations were performed with three codes, PHITS, FLUKA, and GEANT, which had good agreement with the measurements within a factor of 2 for the production rates.

Keywords — High-energy neutrons, shielding experiment, maze, activation detector, Monte Carlo.

Note — Some figures may be in color only in the electronic version.

*E-mail: noriaki.nakao@shimz.co.jp

[†]Present address: Clinique de La Source, Radiation Oncology Institut, Avenue Alexandre-Vinet 30, 1004 Lausanne, Switzerland.

[‡]Present address: National Institutes for Quantum Science and Technology (QST), 6-6-11 Aramaki Aoba, Aoba-ku, Sendai, Miyagi, Japan 980-8579.

[§]Present address: Japan Radioisotope Association, Honkomagome, Bunkyo-ku, Tokyo 113-8941, Japan.

This is an Open Access article distributed under the terms of the Creative Commons Attribution-NonCommercial-NoDerivatives License (<http://creativecommons.org/licenses/by-nc-nd/4.0/>), which permits non-commercial re-use, distribution, and reproduction in any medium, provided the original work is properly cited, and is not altered, transformed, or built upon in any way. The terms on which this article has been published allow the posting of the Accepted Manuscript in a repository by the author(s) or with their consent.

I. INTRODUCTION

A number of particle accelerator facilities have been constructed for physics, medical, and industrial use. Accelerator specifications have been upgraded to enhance the intensity and energy of the particle beam to provide better statistics and more efficient irradiation. To ensure radiation safety in such facilities, the prompt and residual radiation levels should be predicted from the data of secondary neutrons generated by beam irradiation. The neutrons from high-power accelerators are highly penetrative and require a massive shield to suppress the radiation levels outside the facility. As the

radiation shield occupies a considerable portion of the total construction costs, the shielding design is very important when constructing high-intensity and high-energy accelerator facilities. Recently, Monte Carlo simulation have been widely used for the shielding designs in such facilities. Therefore, reliable benchmark experimental data are indispensable for clarifying the accuracy of the simulation results. However, this has not been well validated because reliable experiments are scarcely reported.

In the Takasaki Ion Accelerators for Advanced Radiation Application (TIARA) of the Japan Atomic Energy Research Institute (currently the National Institutes for Quantum and Radiological Science and Technology), 40- and 65-MeV quasi-monoenergetic neutrons have been produced by proton beams, and the neutron energy spectra have been measured behind concrete,¹ iron,² and polyethylene³ shields. At the Alternating Gradient Synchrotron (AGS) in Brookhaven National Laboratory, a shielding experiment with a mercury spallation target bombarded with 24-GeV protons was performed, and attenuation lengths for concrete and iron were experimentally evaluated.⁴ At the High Energy Accelerator Research Organization (KEK) spallation neutron source (KENS) facility using a 500-MeV proton beam, the attenuation of neutrons in the forward direction through the concrete shield was measured.⁵ In the Conseil Européen pour la Recherche Nucléaire (CERN)-European Union High Energy Reference Field (CERF) facility, a 120 GeV/c positive-hadron beam was directed at a thick copper target and the neutron energy spectra between 32 and 380 MeV were measured behind lateral shields of concrete and iron.⁶

A number of measurements of neutron streaming at mazes have also been conducted, but most of them have been for fission neutrons. For high-energy neutrons above

20 MeV, experimental data of maze streaming are very scarce. A measurement of high-energy neutron streaming at a maze was conducted by Tanaka et al.⁷ at the TIARA. In the experiment, neutrons were produced at a thick copper target bombarded by a 68-MeV proton beam, and the neutron energy spectra along the maze were measured using an organic liquid scintillator and Bonner spheres. It was reported that dose-equivalent distributions estimated from the experimental results agreed within a factor of 3 with that calculated by the empirical formula. However, the accuracy of Monte Carlo calculations was not confirmed with the experiment.

This paper reports on the study of experimentally evaluated high-energy neutron fluxes for a lateral shield and a maze at a high-energy proton accelerator facility. At the CERN High-energy Accelerator Mixed-field (CHARM) facility,^{8,9} benchmark experiments of a bulk shield penetration in 2015 (Refs. 10, 11, and 12), a modified shield from 2016 to 2022 (Refs. 13 and 14), and a maze streaming in 2018 (Ref. 15) were performed. The Monte Carlo simulations were carried out and comparisons with the experimental results are discussed.

II. EXPERIMENT

II.A. Facility

Figure 1 shows the horizontal structure of the CHARM facility in the east hall at CERN. The 24 GeV/c protons are transported from the proton synchrotron and injected into a copper target (8-cm diameter × 50-cm thickness) located at the center of the facility. The protons not interacting with the target are transported into an iron beam dump placed

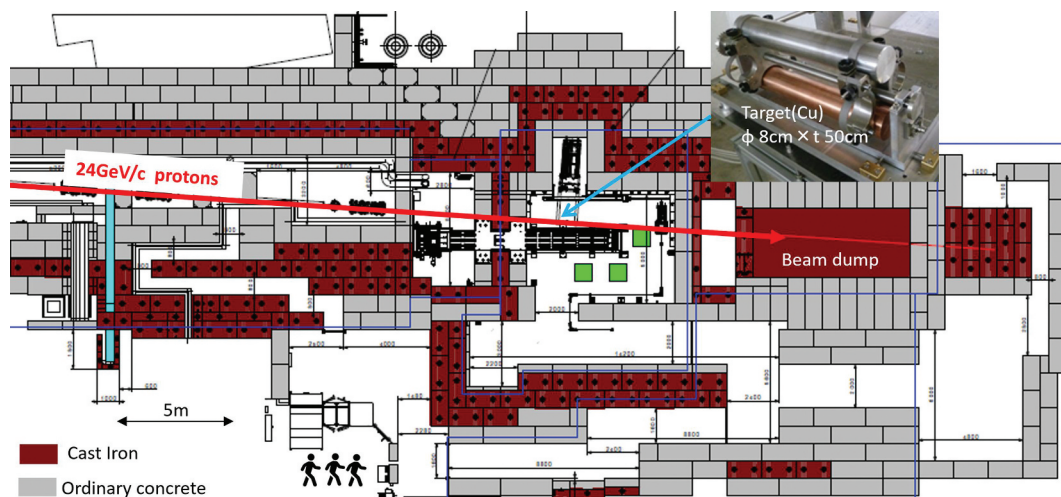


Fig. 1. Horizontal structure of the CHARM facility.

downstream. The proton beam line and target room are surrounded by ordinary concrete and cast-iron shields. The target room can only be accessed through a maze.

Figures 2 and 3 show the vertical shielding structure of the CHARM facility for the original shield structure in 2015 and the one modified at the beginning of 2016, which is perpendicular to the beam axis at the target location. The target center is positioned on the beam line, which is 129 cm above the floor. To the right of the target in Figs. 2 and 3, there is a four-layer movable shield wall of

iron and concrete. Each of the shield layers is 20 cm thick. Above the ceiling of the target room, located 240 cm above the beam line, a bulk shield is constructed of 80-cm-thick cast iron and 360-cm-thick ordinary concrete. A 10-cm-thick marble ceiling is installed 185 cm above the beam line (below the iron ceiling). The densities of the concrete, the cast iron, and the marble of the bulk shield are 2.4, 7.2, and 2.71 g/cm³, respectively.

As shown in the modified shield of Figs. 3 and 4, two setups of the shielding experiment, a removable sample

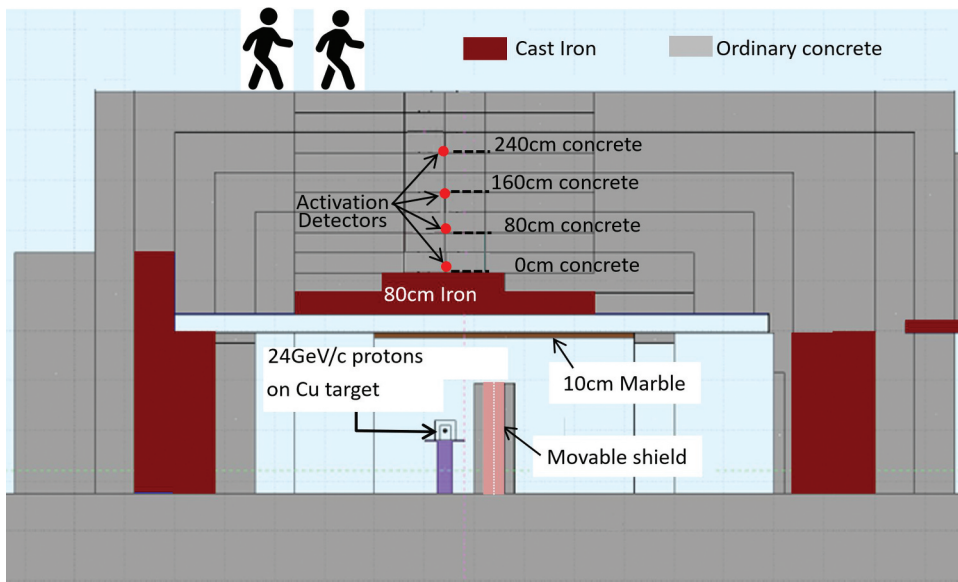


Fig. 2. Vertical cross section of the original shield structure in the CHARM facility perpendicular to the beam axis at the target location. The beam travels from the front to back of this figure.

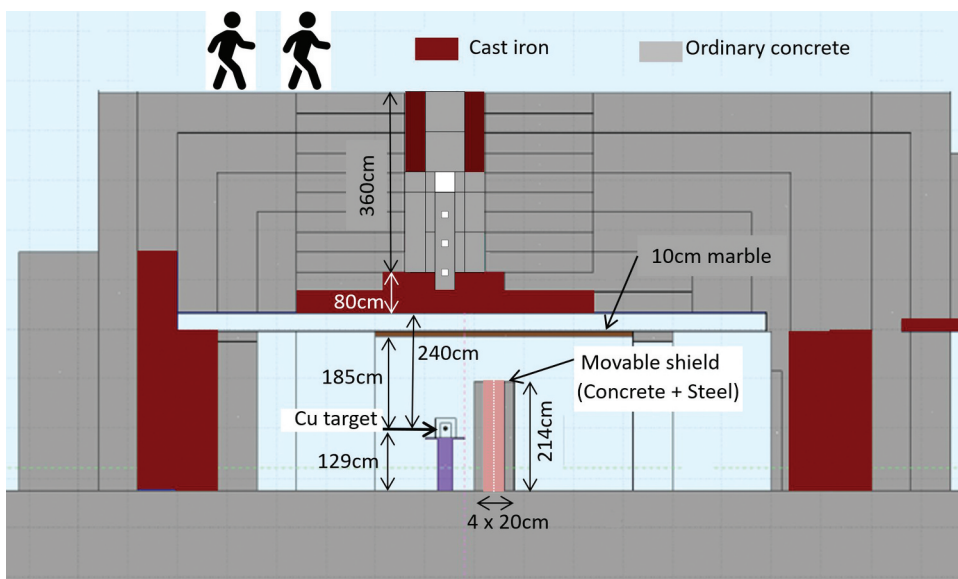


Fig. 3. Vertical cross section of the modified shield structure in the CHARM facility perpendicular to the beam axis at the target location. The beam travels from the front to back of this figure.

block and a material test location, are arranged in the vertical shield just above the target. The removable sample block, made of ordinary concrete with three detector holes at different heights, is placed on a 40-cm-thick iron slab just above the target room ceiling. In the material test location, positioned just above the removable sample block, various test shield blocks can be installed.

II.B. Activation Detector Samples and Experimental Setup

The neutrons transmitted upward through the original bulk shield were measured by activation detector samples composed of bismuth and aluminum, which are widely used in high-energy neutron measurements.¹⁶ The bismuth and aluminum detectors were each prepared in two sizes: 8.0-cm diameter \times 1.0-cm thickness and 4.0-cm diameter \times 0.4-cm thickness. The sample size was varied because the neutron intensity varies inside the shielding. Parts of the concrete blocks were removed from the top of the shield, and the samples were placed at concrete shield depths of 0, 80, 160, and 240 cm, as shown in Fig. 2. After setting the samples, the removed blocks were replaced for the beam irradiation.

For the modified shielding structure shown in Figs. 3 and 4, neutrons were measured using activation detectors of bismuth, aluminum, indium, and graphite, and the two sizes mentioned previously were placed at various shield locations. As shown in Fig. 4a, the samples were placed

at four locations (three holes and the top of the removable block). On the other hand, for the material test location experiment in Fig. 4b and Fig. 4c, samples were placed upon ordinary concrete slabs of 40- to 160-cm thicknesses, and steel slabs of 20- to 80-cm thicknesses were equipped by changing the material and the thickness. The densities of the concrete and the steel of the test shielding material were 2.23 and 7.77 g/cm³, respectively.

The streaming neutrons through the maze were measured by aluminum activation detector of the two sizes, which were varied depending on the neutron intensity. The detectors were placed at 10 locations (Fig. 5) at the beam line height and the horizontal center along the five legs of the maze.

Generally, from the radionuclide production rate in the activation detectors, the attenuation profiles through the various shielding materials were obtained for the reactions of $^{209}\text{Bi}(n,xn)^{210-x}\text{Bi}$ ($x = 4-9$), $^{27}\text{Al}(n,\alpha)^{24}\text{Na}$, $^{115}\text{In}(n,n')^{115m}\text{In}$, and $^{12}\text{C}(n,2n)^{11}\text{C}$.

II.C. Beam Irradiation

The intensity of the 24 GeV/c proton beam at CHARM was 6.7×10^{10} proton/s (Ref. 17) in the maximum. The relative beam intensity was monitored by a secondary emission chamber. In the bulk shielding experiment, the beam irradiation was carried out for about 1 to 18 h, including the night period, depending on the sample. The beam was temporarily stopped after

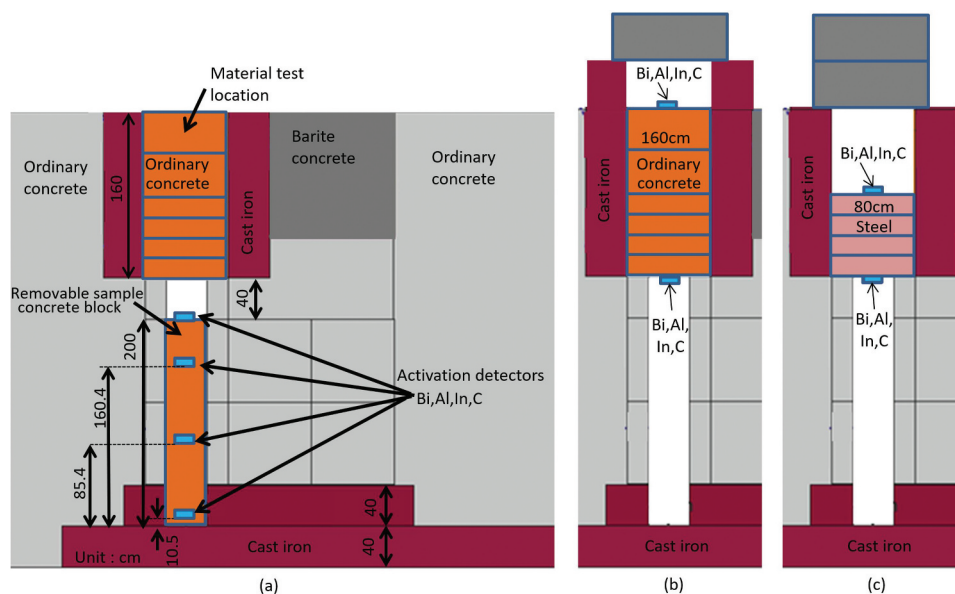


Fig. 4. Locations of the activation detectors and configurations of the measurement in the modified shield structure showing shielding experiments with (a) the removable sample concrete block, and (b) concrete and (c) steel shields in the material test location.

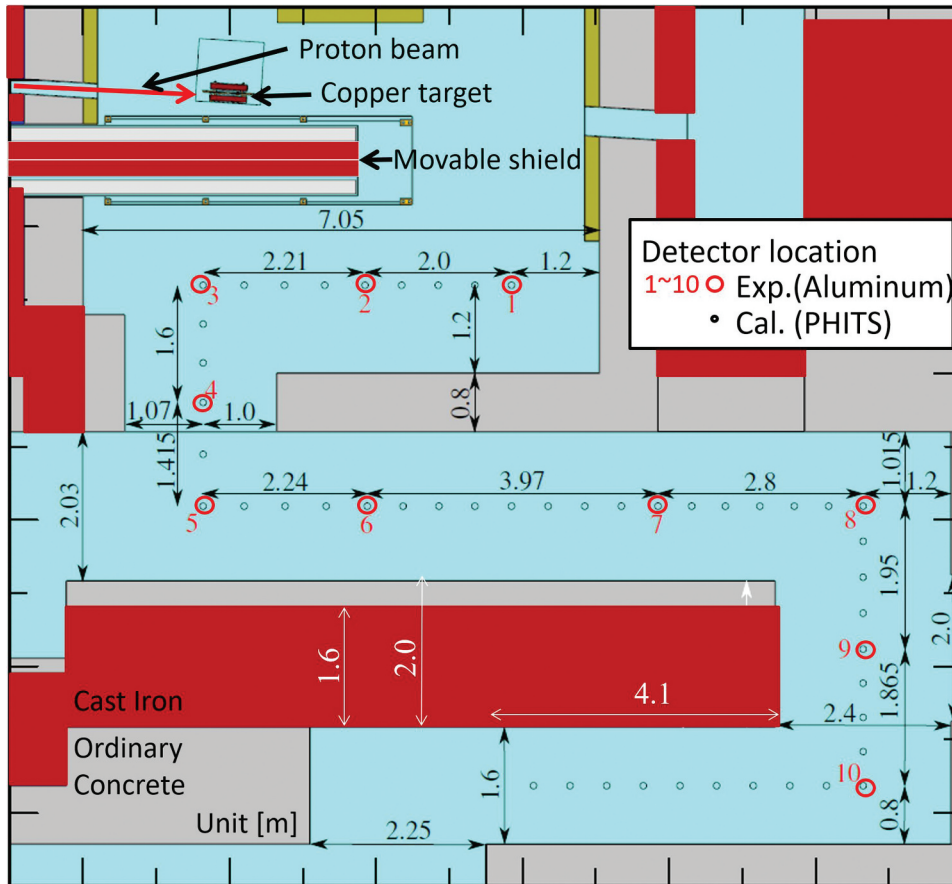


Fig. 5. Maze structure and detector locations.

the irradiation period to remove the irradiated samples and to install new samples at the corresponding locations. In the maze experiment, the beam irradiation was carried out for about 2.5 days over the weekend.

II.D. Radioactivity Measurements

The removed samples were transported to the CERN gamma-spectrometry laboratory, and the energy spectra of the photons from the radionuclides generated in the samples by the $^{209}\text{Bi}(n,xn)^{210-x}\text{Bi}$ (where $x = 4$ to 9), $^{27}\text{Al}(n,\alpha)^{24}\text{Na}$, $^{115}\text{In}(n,n')^{115m}\text{In}$, $^{27}\text{Al}(n,\alpha)^{24}\text{Na}$, and $^{12}\text{C}(n,2n)^{11}\text{C}$ reactions were measured by a high-purity germanium-semiconductor detector (Ge-detector). To estimate the radioactivity of the corresponding nuclides with short (^{201}Bi and ^{202}Bi), medium (^{203}Bi and ^{204}Bi), and long (^{205}Bi and ^{206}Bi) half-lives, the bismuth samples were measured continuously three times for 3, 15, and 24 h, respectively. The aluminum samples were measured for times between 3 and 24 h, depending on the peak count rates of the photons from ^{24}Na . For others,

measuring times were 4 h for the indium samples and 15 to 30 min for the graphite samples.

II.E. Data Analysis

Table I lists the analyzed radionuclide production reactions, half-lives, and photon energies with their emission ratios. The net counts of the photopeak at the corresponding photon energies were analyzed, and the production rates of the radionuclides in the activation detector samples per proton beam irradiation were estimated from the photopeak efficiencies of the Ge-detector and the beam intensity fluctuations during the irradiation. The efficiencies of the Ge-detector were estimated in LabSOCS software¹⁸ (Mirion Technologies, Canberra KK).

III. MONTE CARLO SIMULATIONS

A Monte Carlo simulation was performed with the Particle and Heavy Ion Transport code System¹⁹ (PHITS) Version 3.02 to simulate neutron flux distribution in the

TABLE I
Production Reactions, Half-Lives, and Photon Energies of the Radionuclides in the Activation Detectors

Reaction	Half-Life	Photon Energy [keV] (Emission Ratio)		
$^{115}\text{In}(n,n')^{115m}\text{In}$	4.486 h	336.0 (0.458)		
$^{27}\text{Al}(n,\alpha)^{24}\text{Na}$	14.96 h	1368.6 (1.000)	2754.6 (0.999)	
$^{12}\text{C}(n,2n)^{11}\text{C}$	20.39 min	511.0 (1.995)		
$^{209}\text{Bi}(n,4n)^{206}\text{Bi}$	6.24 day	803.1 (0.989)	881.0 (0.662)	1718.7 (0.318)
$^{209}\text{Bi}(n,5n)^{205}\text{Bi}$	15.31 day	703.4 (0.310)	1764.4 (0.325)	
$^{209}\text{Bi}(n,6n)^{204}\text{Bi}$	11.22 h	899.2 (0.988)	984.0 (0.593)	
$^{209}\text{Bi}(n,7n)^{203}\text{Bi}$	11.76 h	820.2 (0.297)	825.3 (0.146)	1847.4 (0.114)
$^{209}\text{Bi}(n,8n)^{202}\text{Bi}$	1.72 h	422.2 (0.837)	657.5 (0.606)	960.7 (0.994)
$^{209}\text{Bi}(n,9n)^{201}\text{Bi}$	1.80 h	629.1 (0.240)		

original bulk shield. For the reactions of neutrons above 20 MeV and protons, the evaporation model GEM (Ref. 20) was used; for neutrons up to 3 GeV, the intra-nuclear cascade model INCL (Ref. 21) was used; and for high-energy nuclear reactions above 3 GeV, the JAM model²² was used in the PHITS code. For neutrons below 20 MeV, the JENDL-4.0 data library²³ was used.

Since the structure of the original upper bulk shield in this facility was comparatively simple and wide, the calculation of two steps was performed with a simplified geometry to shorten the calculation time. First, the angular and energy spectra of the neutrons above 1 MeV produced from the copper target injected by the 24 GeV/c proton beam were simulated. The obtained

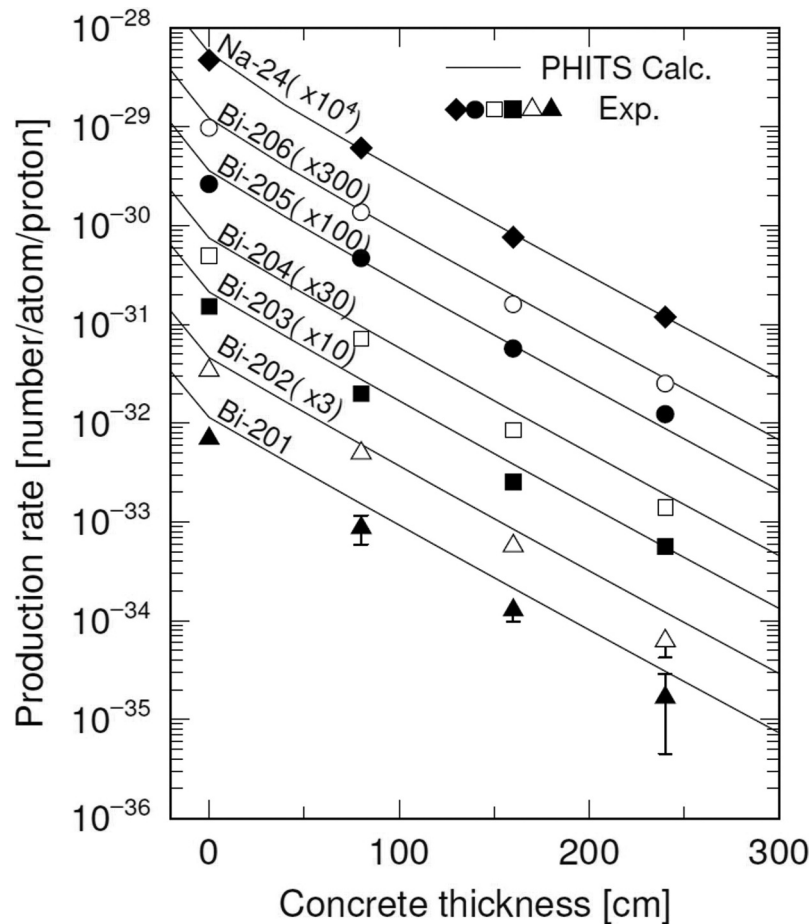


Fig. 6. Comparison of experimental and simulated attenuation profiles of the radionuclide production rates in the original shield structure in the CHARM facility.

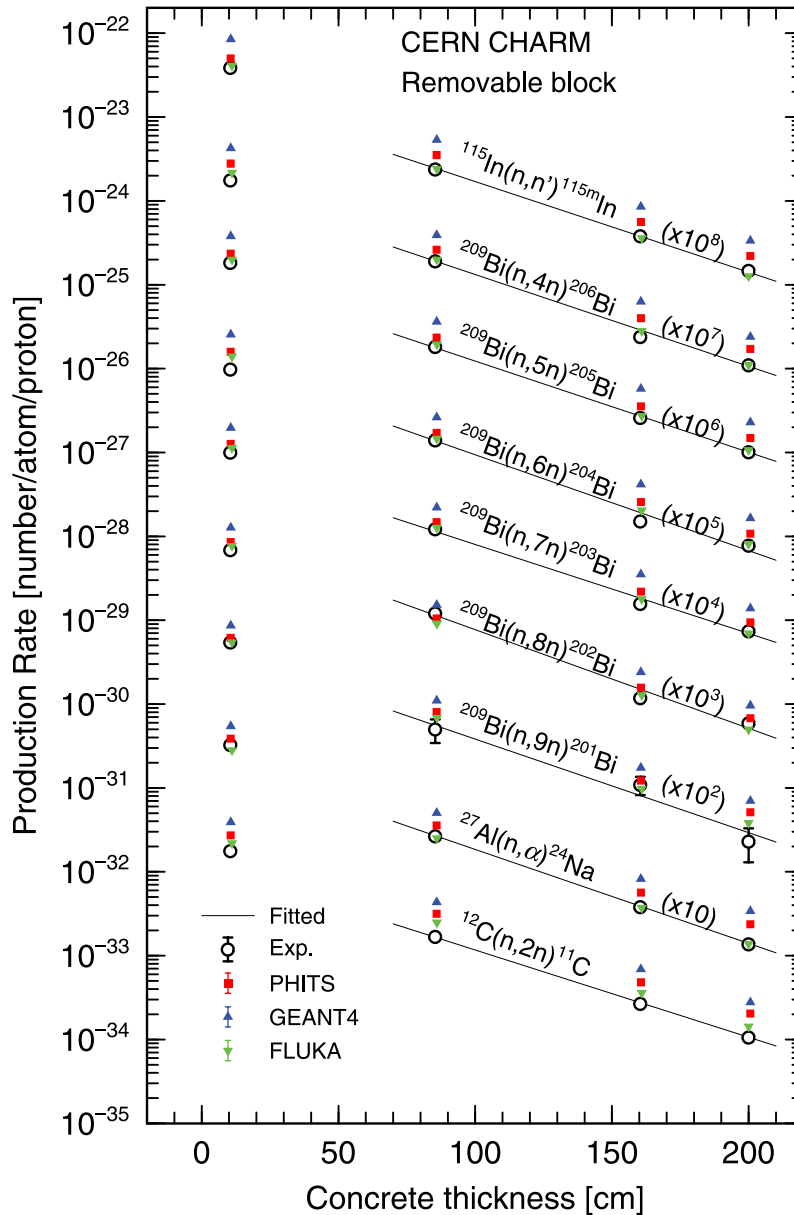


Fig. 7. Attenuation profile of experimental and calculated production rates as a function of concrete thickness for the removable block configuration.

energy spectrum at 90 deg was chosen as the source term for the second-step calculation with the deep shield. Disk-shaped slabs with a sufficiently wide radius (10 m), including a 10-cm-thick marble, an 80-cm-thick iron, and 800-cm-thick concrete were placed in order from the source position.

A pencil beam of the source neutrons was injected into the center of the marble slab. To ensure good neutron statistics in the deep-shield region, a variance reduction technique (importance method) was applied in the second-step calculation. Using surface-crossing estimators in a 40-cm-thick interval in the concrete, the neutrons in the whole planes of

the 10-m radius at the same depths were integrated, and the neutron energy spectra were estimated. This method was equivalent to the one-dimensional calculation for a plane source. The absolute values of the energy spectra were finally divided by the square of distances between the target and the corresponding estimator planes to obtain the results as a point source.

For the modified shielding structure, Monte Carlo simulations were performed with the FLUctuating KASKade code (FLUKA) version 4-2.2 distributed by the FLUKA.CERN collaboration,^{24,25} the PHITS version 3.24, and the GEometry ANd Tracking (GEANT) version 4.10.07-02

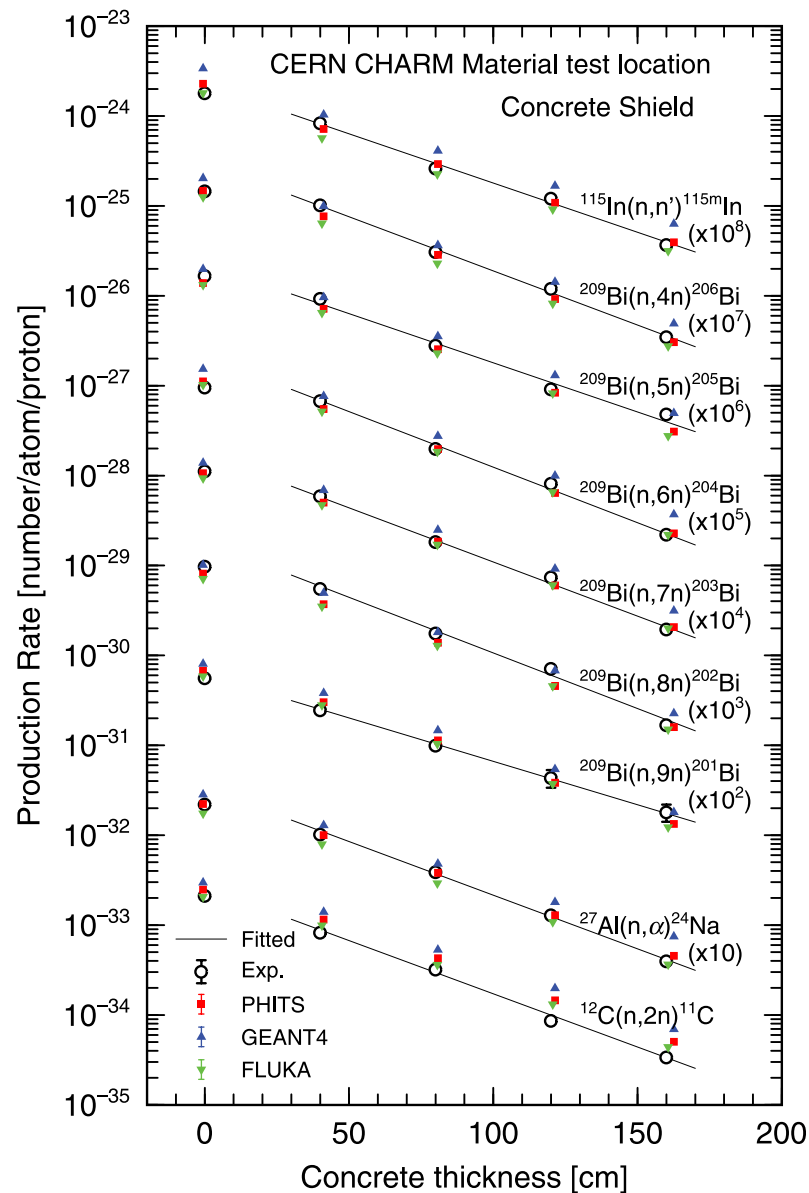


Fig. 8. Attenuation profile of experimental and calculated production rates as a function of concrete thickness in the material test location.

(Refs. 26 and 27). In the simulations, the geometries of the detailed shield structure were described. A track-length estimator was used for scoring the particle in the detector regions to estimate particle fluxes. An importance method for the variance reduction technique was also used to get better statistics. For all simulations, the energy spectra of the scored particles were estimated above thermal energy for FLUKA, 0.1 MeV for PHITS, and 0.315 MeV for GEANT4 calculations.

Simulations for the maze were performed with PHITS version 3.10 and FLUKA. The geometries of the detailed

shield structure, shown in Fig. 5, were described in the simulations. The neutron energy spectra were obtained using track-length estimators that were placed at the horizontal center of the maze at the beam line height along the five legs. The locations of these estimators included the corresponding 10 experimental positions.

The radionuclide production rates were estimated by folding (multiplying and integrating) the simulated energy spectra with the cross-section data for $^{209}\text{Bi}(n, x\text{n})^{210-x}\text{Bi}$ ($x = 4-9$), $^{27}\text{Al}(n, \alpha)^{24}\text{Na}$, $^{115}\text{In}(n, n')^{115m}\text{In}$, and $^{12}\text{C}(n, 2\text{n})^{11}\text{C}$ evaluated by Maekawa et al.²⁸

IV. RESULTS AND DISCUSSIONS

The experimental attenuation profiles of the radionuclide production rates through the original bulk shield are shown in Fig. 6, and those through the modified shield structure are shown in Figs. 7, 8, and 9, while those along the maze are shown in Fig. 10. The errors in these figures are the statistical errors of the photon counting data. The uncertainties in the Ge-detector efficiency by LabSOCS (Ref. 18) and the beam monitor calibration¹⁰ (4.3% and 7%, respectively) are not included in the figures. For comparison, the simulation results are also shown in the figures.

In Fig. 6, the production rates decreased exponentially with increasing depth through the original bulk shield. The simulated production rates generally agreed with the measured values, especially for ^{24}Na and ^{206}Bi . The simulated and experimental production rates of ^{24}Na and ^{206}Bi agreed within ~20%, and those of ^{205}Bi , ^{204}Bi , and ^{203}Bi agreed within 30% to 50%. Although the simulated production rates of ^{202}Bi and ^{201}Bi showed overestimation, they deviated within a factor of 2 from the measured rates.

For the modified shielding structure, simulated production rates were compared with the experimental data, as shown in Figs. 7, 8, and 9 for the removable block,

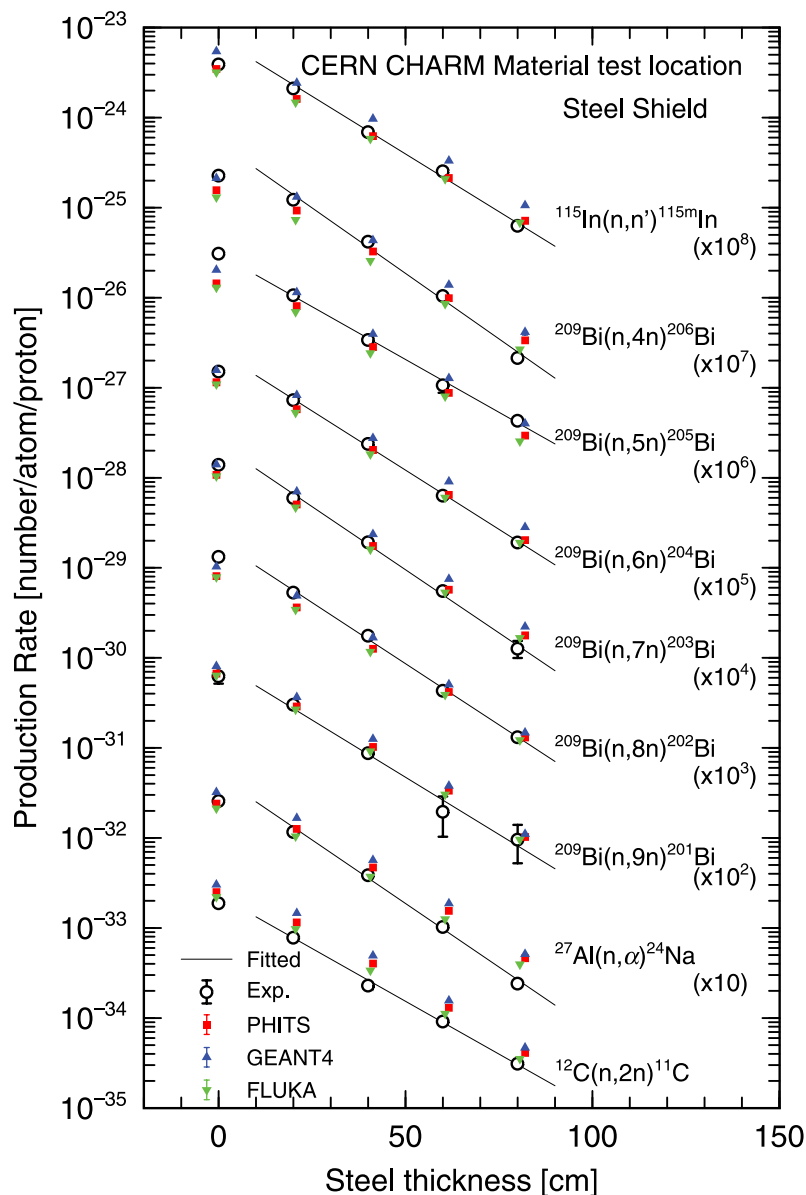


Fig. 9. Attenuation profile of experimental and calculated production rates as a function of steel thickness in the material test location.

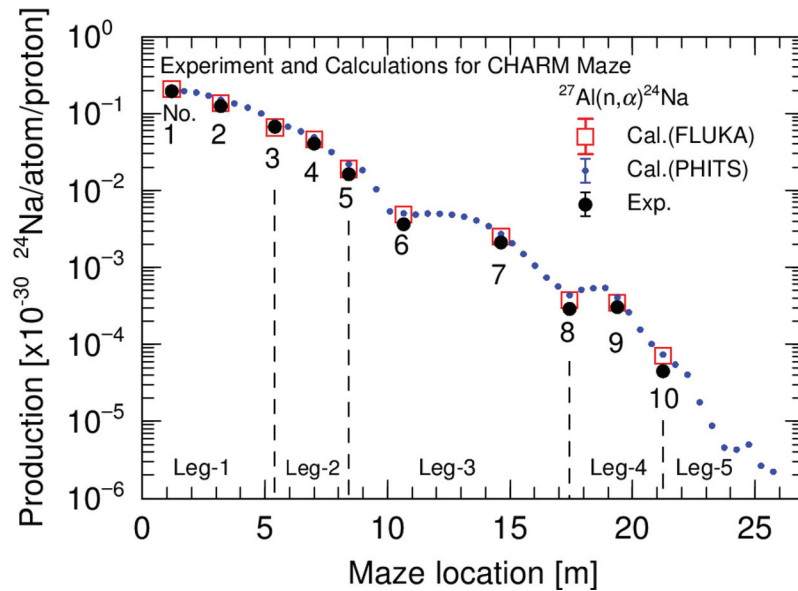


Fig. 10. Attenuation profile of experimental production rates along the maze compared with the calculated ones.

concrete, and steel shield, respectively. For the removable block, FLUKA gave good agreement with the experiment within around 10%. On the other hand, overestimations by 35% to 60% for PHITS and by a factor of 2 for GEANT4 can be found. For the concrete and steel shields, agreements can be seen within 30% for FLUKA, within 20% for PHITS, and within 40% for GEANT4.

For the maze streaming shown in Fig. 10, it is observed that the ^{24}Na production rates decreased with the distance from the target along the maze. The simulated production rates generally agreed with the measured values, especially in the first and second legs. Although overestimations of the simulation can be seen in the third and fourth legs, the discrepancies are up to a factor of 2. Around experimental location 9, higher production rates than those around location 8 can be observed both in the experimental and simulated data. It was clarified by the simulation that this phenomenon is caused by a contribution of high-energy neutrons penetrating a direct path through the 0.8-m-thick shield between the first and third legs.

V. CONCLUSION

The attenuation of neutrons through the original bulk concrete shield, various thicknesses of the concrete and steel shields, and along the maze were measured using activation detectors in the CHARM facility at CERN with a 24 GeV/c proton beam. The radionuclide production rates of the ^{209}Bi (n, xn) $^{210-x}\text{Bi}$ ($x = 4-9$), $^{27}\text{Al}(n, \alpha)^{24}\text{Na}$, $^{115}\text{In}(n, n')^{115m}\text{In}$, and

$^{12}\text{C}(n, 2n)^{11}\text{C}$ reactions were measured. The results of Monte Carlo simulations reasonably agreed with the measured data within a factor of 2. This work provides useful benchmark experimental data for a deep-shield penetration and maze streaming in a high-energy proton accelerator facility. The results are expected to improve our understanding of shielding design in future high-energy accelerator facilities.

Acknowledgments

The authors are deeply grateful to the accelerator operation staff and the experimental groups at the IRRAD and the CHARM facilities for their helpful support with the experiment. They are also grateful to the staff of the gamma-spectrometry laboratory at CERN for their support in the measurement and analysis of the Ge-detectors.

Disclosure Statement

No potential conflict of interest was reported by the authors.

ORCID

Noriaki Nakao <http://orcid.org/0000-0002-5910-8222>
 Toshiya Sanami <http://orcid.org/0000-0003-2255-8008>
 Tsuyoshi Kajimoto <http://orcid.org/0009-0003-6133-3888>
 Robert Froeschl <http://orcid.org/0000-0002-2194-5869>
 Davide Bozzato <http://orcid.org/0000-0001-5306-361X>

Elpida Iliopoulou  <http://orcid.org/0000-0003-0895-9227>
 Angelo Infantino  <http://orcid.org/0000-0002-7854-3502>
 Hiroshi Yashima  <http://orcid.org/0000-0003-0931-5984>
 Eunji Lee  <http://orcid.org/0000-0002-0600-2571>
 Takahiro Oyama  <http://orcid.org/0000-0002-9425-0275>
 Masayuki Hagiwara  <http://orcid.org/0000-0003-0236-2905>
 Tetsuro Matsumoto  <http://orcid.org/0000-0003-2047-7028>
 Akihiko Masuda  <http://orcid.org/0000-0003-0572-0341>
 Yoshitomo Uwamino  <http://orcid.org/0000-0002-8359-3520>
 Stefan Roesler  <http://orcid.org/0000-0002-5920-0459>
 Markus Brugger  <http://orcid.org/0000-0002-3645-7091>

References

1. N. NAKAO et al., “Transmission Through Shields of Quasi-Monoenergetic Neutrons Generated by 43- and 68-MeV Protons: Part I—Concrete Shielding Experiment and Calculation for Practical Application,” *Nucl. Sci. Eng.*, **124**, 228 (1996); <https://doi.org/10.13182/NSE96-A28574>.
2. H. NAKASHIMA et al., “Transmission Through Shields of Quasi-Monoenergetic Neutrons Generated by 43- and 68-MeV Protons: Part II—Iron Shielding Experiment and Analysis for Investigating Calculation Methods and Cross Section Data,” *Nucl. Sci. Eng.*, **124**, 243 (1996); <https://doi.org/10.13182/NSE96-A28575>.
3. N. NAKAO et al., “Measurements and Calculations of Neutron Energy Spectra Behind Polyethylene Shields Bombarded by 40- and 65-MeV Quasi-Monoenergetic Neutron Sources,” *J. Nucl. Sci. Technol.*, **34**, 4, 348 (1997); <https://doi.org/10.1080/18811248.1997.9733674>.
4. H. NAKASHIMA et al., “Research Activities on Neutronics Under ASTE Collaboration at AGS/BNL,” *J. Nucl. Sci. Technol.*, **39**, Supplement 2, 1155 (2002); <https://doi.org/10.1080/00223131.2002.10875307>.
5. N. NAKAO et al., “Arrangement of High-Energy Neutron Irradiation Field and Shielding Experiment Using 4 M Concrete at KENS,” *Proc. 10th Int. Conf. on Radiation Shielding (ICRS10)*, pp. 553–557, Madeira, Portugal, May 9–14, 2004 (2005).
6. N. NAKAO et al., “Measurement and Calculation of High-Energy Neutron Spectra Behind Shielding at the CERF 120 GeV/c Hadron Beam Facility,” *Nucl. Instr. Meth. B*, **266**, 93 (2008); <https://doi.org/10.1016/j.nimb.2007.09.043>.
7. S. TANAKA et al., “An Experimental Study on Radiation Streaming Through a Labyrinth in a Proton Accelerator Facility of Intermediate Energy,” *Health Phys.*, **81**, 4, 406 (2001); <https://doi.org/10.1097/00004032-200110000-00005>.
8. R. FROESCHL, “Radiation Protection Assessment of the Proton Irradiation Facility and the CHARM Facility in the East Area,” Technical Report CERN-RP-2014-008-REPORTS-TN, EDMS 1355933, Conseil Européen pour la Recherche Nucléaire (2014).
9. R. FROESCHL, M. BRUGGER, and S. ROESLER, “The CERN High Energy Accelerator Mixed Field (CHARM) Facility in the CERN PS East Experimental Area,” *Proc. SATIF12, NEA/NSC/R(2015)*, p. 14, Batavia, Illinois (2014).
10. E. ILIOPOULOU et al., “Measurements and FLUKA Simulations of Bismuth and Aluminum Activation at the CERN Shielding Benchmark Facility (CSBF),” *Nucl. Instr. Meth.*, **A855**, 79 (2018); <https://doi.org/10.1016/j.nima.2017.12.058>.
11. T. KAJIMOTO et al., “Neutron Energy Spectrum Measurement Using an NE213 Scintillator at CHARM,” *Nucl. Instr. Meth.*, **B429**, 27 (2018); <https://doi.org/10.1016/j.nimb.2018.05.024>.
12. N. NAKAO et al., “Attenuation Length of High Energy Neutrons Through a Thick Concrete Shield Measured by Activation Detectors at CHARM,” *J. Nucl. Sci. Technol.*, **57**, 9, 1022 (2020); <https://doi.org/10.1080/00223131.2020.1751740>.
13. E. ILIOPOULOU et al., “Measurements and FLUKA Simulations of Bismuth and Aluminum Activation at the CERN Shielding Benchmark Facility (CSBF),” *Nucl. Instr. Meth.*, **A855**, 79 (2018).
14. E. LEE et al., “Energy Spectra of Neutrons Penetrating Concrete and Steel Shielding Blocks from 24 GeV/c Protons Incident on Thick Copper Target,” *Nucl. Instr. Meth.*, **A998**, 165189 (2021); <https://doi.org/10.1016/j.nima.2021.165189>.
15. N. NAKAO et al., “Measurements and Monte Carlo Simulations of High-Energy Neutron Streaming Through the Access Maze Using Activation Detectors at 24 GeV/c Proton Beam Facility of CERN/CHARM,” *J. Nucl. Sci. Technol.*, **58**, 8, 899 (2021); <https://doi.org/10.1080/00223131.2021.1887003>.
16. N. NAKAO, Y. UWAMINO, and K. TANAKA, “Measurement of the Neutron Angular Distribution from a Beryllium Target Bombarded with a 345-MeV/u ^{238}U Beam at the RIKEN RI Beam Factory,” *Nucl. Instr. Meth.*, **B423**, 27 (2018); <https://doi.org/10.1016/j.nimb.2018.02.036>.
17. L. GATIGNON, “Beam Properties for the East Area Irradiation Facility in the T8 Beam Line,” Technical Report EAT8, EDMS, CERN 1270807 (2013).

18. F. L. BRONSON, “Validation of the Accuracy of the LabSOCS Software for Mathematical Efficiency Calibration of Ge Detectors for Typical Laboratory Samples,” *J. Radioanal. Nucl. Chem.*, **255**, 137 (2003); <https://doi.org/10.1023/A:1022248318741>.
19. T. SATO et al., “Features of Particle and Heavy Ion Transport Code System PHITS Version 3.02,” *J. Nucl. Sci. Technol.*, **55**, 684 (2018); <https://doi.org/10.1080/00223131.2017.1419890>.
20. S. FURIHATA, “Statistical Analysis of Light Fragment Production from Medium Energy Proton-Induced Reactions,” *Nucl. Instrum. Meth. B*, **171**, 251 (2000); [https://doi.org/10.1016/S0168-583X\(00\)00332-3](https://doi.org/10.1016/S0168-583X(00)00332-3).
21. A. BOUDARD et al., “New Potentialities of the Liège Intranuclear Cascade Model for Reactions Induced by Nucleons and Light Charged Particles,” *Phys. Rev. C*, **87**, 014606 (2013); <https://doi.org/10.1103/PhysRevC.87.014606>.
22. Y. NARA et al., “Relativistic Nuclear Collisions at 10A GeV Energies from p+Be to Au+Au with the Hadronic Cascade Model,” *Phys. Rev. C*, **61**, 2, 024901 (2000); <https://doi.org/10.1103/PhysRevC.61.024901>.
23. K. SHIBATA et al., “JENDL-4.0: A New Library for Nuclear Science and Engineering,” *J. Nucl. Sci. Technol.*, **48**, 1 (2011); <https://doi.org/10.1080/18811248.2011.9711675>.
24. C. AHDIDA et al., “New Capabilities of the FLUKA Multi-Purpose Code,” *Front. Phys.*, **9**, 788253 (2022); <https://doi.org/10.3389/fphy.2021.788253>.
25. G. BATTISTONI et al., “Overview of the FLUKA Code,” *Ann. Nucl. Energy*, **82**, 10 (2015); <https://doi.org/10.1016/j.anucene.2014.11.007>.
26. J. ALLISON et al., “Recent Developments in GEANT4,” *Nucl. Instr. Meth.*, **A835**, 186 (2016); <https://doi.org/10.1016/j.nima.2016.06.125>.
27. S. AGOSTINELLI et al., “Geant4—A Simulation Toolkit,” *Nucl. Instr. Meth. A*, **506**, 250 (2003); [https://doi.org/10.1016/S0168-9002\(03\)01368-8](https://doi.org/10.1016/S0168-9002(03)01368-8).
28. F. MAEKAWA et al., “Production of a Dosimetry Cross Section Set Up to 50 MeV,” *Proc. 10th Int. Symp. on Reactor Dosimetry*, p. 417, Osaka, Japan, September 12–17, 1999, American Society for Testing and Materials (2001).